A COMPARATIVE EVALUATION AND ANALYSIS OF FREE-FORM SURFACE DEVIATIONS USING ARTICULATED ARM CMM AND 3D SCANNER

Rahul MALI[1], T V K GUPTA[2*]

The machined parts should confer specified quality standards to perform their intended functions effectively. CMM and 3D scanners are the commonly employed inspection devices to determine accuracy, precision, and tolerance. A simple statistical approach is presented in this work to inspect surface deviations using CMM and 3D scanner. The inspection data is statistically evaluated in terms of average deviations, range, standard deviations using both devices and presented in the form of normal distribution. Accordingly, the study quantifies and compares the 'accuracy' and 'precision' of measurements. The result shows that, although 3D scanner inspections are faster, CMM data is more accurate and precise.

Keywords: Free-form surface inspection, Surface deviation, CMM, 3D Scanner, Inspection accuracy.

1. Introduction

Free-form surfaces are the most common in a variety of industrial applications like die/molds, patterns, automotive components, plastic products and household appliances, etc. These surfaces not only facilitate better product aesthetics but also enhances the operating capability or functionality [1]. A free-form surface is featured with varying dimensions and geometries along three principal axes that pose challenges to machine accurately followed by inspection [2]. The machined surfaces often deviate from the desired dimensions which are precisely evaluated with state-of-the-art inspection devices. A precision inspection relies on either contact type devices like gauges, CMM, etc., or non-contact type like laser/optic based devices. The other essential elements of the inspection process like surface data acquisition, sampling strategies (inspection path planning), surface localization, geometric description of the acquired data and form error evaluation, etc., are discussed by Mali et al. and Li et al. [3,4]. The adequate number of measurement points [5], effective sampling strategy [6] followed by accurate surface fitting or reconstruction [7,8] (part registration) by

[1] Assistant Prof., Pimpri Chinchwad College of Engineering Pune, INDIA e-mail: malirahul@hotmail.com
[2]* Associate Prof., Visvesvaraya National Institute of Technology Nagpur, INDIA e-mail: tvkgup@gmail.com (corresponding author)

superimposing the measured surface to CAD model and evaluating the form errors are significant steps in the part inspection process. A CMM and 3D scanner are the most widely used contact and non-contact type devices.

In the past decade, CMMs became an indispensable part of manufacturing industries that require high machining complexities, acute tolerance requirements, availability and affordability with user-friendly interface [3,6]. These devices being featured with high accuracy, precision, and repeatability are used for a broad spectrum of inspections, especially in mass production like automotive parts and general mechanical components, etc. [5]. One of the active research fields of CMM evaluations is to determine the effective sampling strategy and inspection path, where the adequate number of measurement points are strategically distributed across the surface. Several algorithms/models are developed and accordingly, more sample points are allotted in critical regions to ensure that surface reconstruction fulfils the accuracy criteria with minimum time and expense [9,10]. The authors presented a review on different sampling strategies (sample size and point distribution) on part inspection process [6]. Rajamohan et al. [9] ensured proper point distribution based on surface geometric characteristics like curve length and surface area. The surface errors are accurately simulated considering different types of deviations that occurs during machining. Zahmati et al. [10] implemented the particle swarm optimization (PSO) for minimizing form error with an improved (hybrid) sampling strategy. The authors developed a probe tip radius correction algorithm to ensure the free-form surface reconstruction accuracy maintaining the error range in ±0.02 mm [7]. Besides ensuring efficient sampling and path planning, few researchers extended their efforts to understand the error sources considering process uncertainties. Such an approach enables to anticipate the errors and proactively implement corrective measures in CMM and laser-based measurements [11,12].

Further, the laser or optic based devices used in reverse engineering applications for scanning complicated geometries are integrated to transfer them into 3D models [13]. The research community at large established the proficiency of these devices in part inspection to evaluate form error [14,15]. Several authors attempted to enhance the accuracy of these devices by controlling the error sources [11,16] and appropriately set the significant parameters like scanning speed and path, stand-off distance, relative position (orientation) of a scanning probe, etc., that governs overall inspection quality [17,18]. The effectiveness of a reverse engineering methodology in accurately evaluating the turbine blade surfaces employing optical and CT (X-ray) scanners is discussed. The uncertainty values for these devices are analyzed and the acquired measurements are confirmed with modular free-form gauges [15]. Lee et al. evaluated and optimized the inspection path for free-form shape scanning ensuring minimum scanning time. The algorithm calculates the required number of scans along with the most

desirable scan direction within the constraints. Further, the authors developed an efficient hardware and software system to facilitate automated laser scanning and inspection of free-form surfaces. The optimal scan paths are generated by correctly setting different scanning parameters, and the measurement quality is verified by comparing point data with the CAD model [13,19]. The authors evaluated the efficiency of various digitizing methods ensuring measurement accuracy for turbine blade air foil [14]. Chen and Shang [20] performed inspection path optimization using genetic algorithm (GA), particle swarm optimization (PSO) and ant colony optimization algorithms on free-form surfaces. An effective measurement strategy along with an error-compensation model is presented by Li et al. [16] for in-situ inspection of free-form surfaces using a laser sensor. The influence of different parameters like scan depth, incident and azimuth angles, etc., are investigated to enhance the measurement accuracy by setting the orientation and sensor position. A systematic error correction strategy for laser-based measurements and the effect of distance, incidence and projected angles is discussed. Further, the authors defined the relative orientation and position of sensor with respect to part surface and optimized them considering measurement uncertainties [21].

Moreover, integration of both contact and non-contact devices to formulate a multisensory approach for effective surface inspection is also attempted. Here, parts are initially scanned by a laser/vision system to identify the surface characteristics and accordingly, an efficient inspection path is determined; so, this approach assimilates benefits of both CMM and laser scanners with increased inspection accuracy and speed [22,23]. However, comparison of both the methods (CMM and scanner-based) in terms of statistical parameters for free-form surfaces is not fully attempted. The present literature has focused on the measurement accuracy; however, here the authors considered measurement 'precision' also that describes the data distribution. This work attempts to analyse and compare the accuracy and precision of CMM and lased based measurements for free-form surface inspection.

2. Experimentation and Inspection Methodology

2.1. Experimental details

Aluminium 7075 alloy having good fatigue strength, moderate toughness, and high strength to weight ratio is widely used in aerospace and aircraft industries [24]. Fig. 1 shows the experimental set-up along with the step involved in free-form surface machining process. Al-7075 metal block of size 78 × 30 × 26 mm is fixed on a dynamometer using a fixture plate with allen bolts (M8 × 1.0 mm) as shown in Fig. 1 (b). A total of nine experiments are performed based on the Taguchi L_9 array that gives nine free-form samples for inspection. All the

experiments are performed on a 3-axis CNC machine with Siemens (Sinumerik 808D) controller. This milling center is equipped with 10000 rpm maximum spindle speed, 4 μm repeatability and 5 μm positioning accuracy. Each part is accomplished in two steps i.e., firstly the roughing operation employing a flat-end mill and later the finishing experiments with a ball-end cutter.

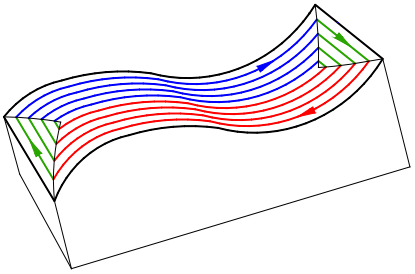

(a) Part CAD model (with tool-path)

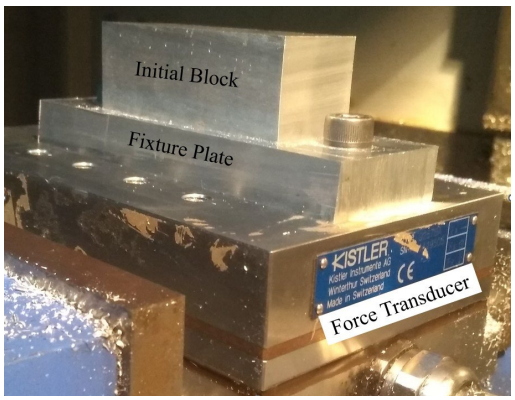

(b) Experimental setup

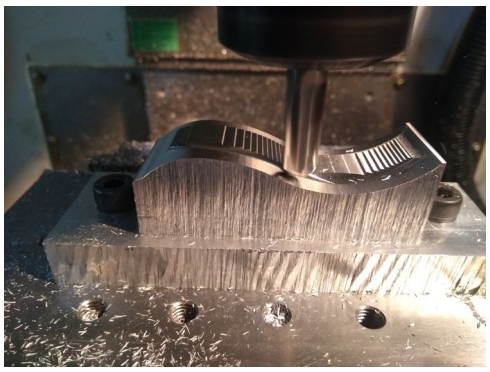

(c) Semi-finished part

(d) Finished part

Fig. 1. Free-form surface finishing process.

Table 1

Process parameters for roughing expt.

V_c (m/min)	f (mm/rev)	a_p (mm)	a_e (mm)
170	0.2	0.6	8

Fig. 1 (c) depicts a semi-finished surface featured with feed marks/machining steps obtained in roughing cut. 3D offset strategy [1] (shown in Fig. 1 (a)) is employed to carry out the finishing cut, which removes the leftover material to generate the final finished surface, shown in Fig. 1 (d). The part is modelled in PTC CREO parametric-3.0 and the NC tool path is generated with

Delcam Power-Mill 16.0 software: simulating the tool-paths in Power mill before actual experimentation. The roughing and finishing operations are carried out with an uncoated carbide, 4 flute flat and ball end of 12 mm and 10 mm dia. respectively, having a helix angle of 30°. The machining parameters i.e., spindle speed (V_c), feed (f), axial (a_p) and radial (a_e) depth of cut for all nine roughing cuts are kept constant (same), while the parameters for all nine finishing experiments (Taguchi L_9 array) are listed in Tables 1 and 2, respectively.

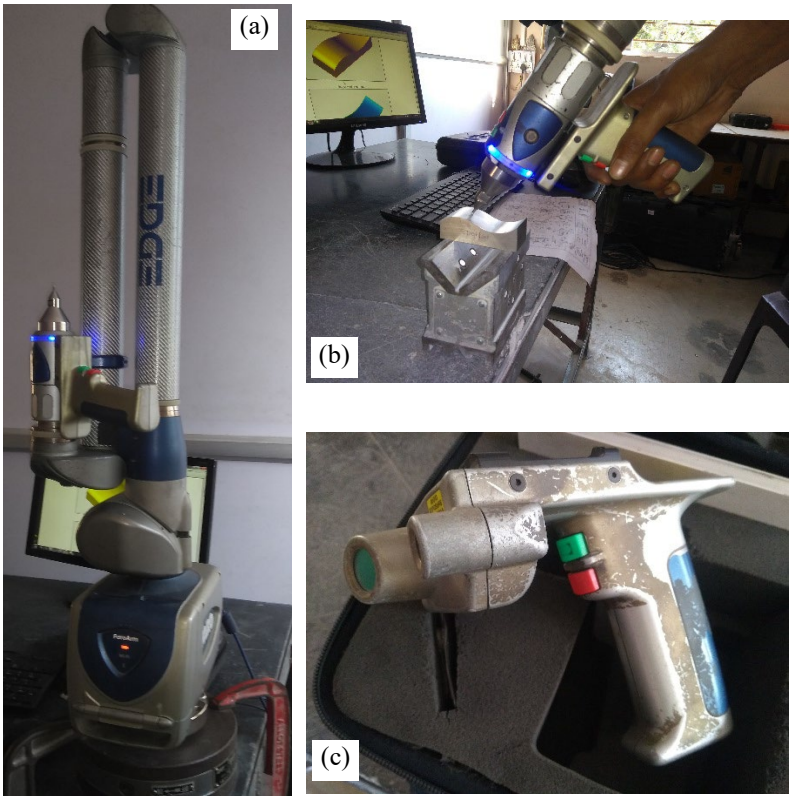

Fig. 2. (a) Inspection set-up including, (b) Articulated CMM (c) 3D Scanner.

Table 2

Process parameters and results (in micrometer) for L_9 experiments

Expt. No.	Vc (m/min)	f (mm/rev)	a_p (mm)	Avg. Dev. (CMM)	Avg. Dev. (Scan)	Range (CMM)	Range (Scan)	Std. Dev. (CMM)	Std. Dev. (Scan)
1.	47	0.05	0.2	5.4	8.7	26	42	6.69	10.56
2.	47	0.1	0.4	3.5	4.3	20	24	4.46	5.39
3.	47	0.15	0.6	4	8.8	22	47	5.36	10.91
4.	94	0.05	0.4	2.8	5.4	16	24	3.59	6.46
5.	94	0.1	0.6	3.9	6.4	20	37	5.08	8.04

6.	94	0.15	0.2	3.8	5.4	18	27	4.59	6.69
7.	141	0.05	0.6	5.1	6	22	35	6.16	7.79
8.	141	0.1	0.2	4.5	4.8	23	26	5.69	6.03
9.	141	0.15	0.4	2.6	6.8	16	27	3.45	7.95

2.2. Inspection methodology

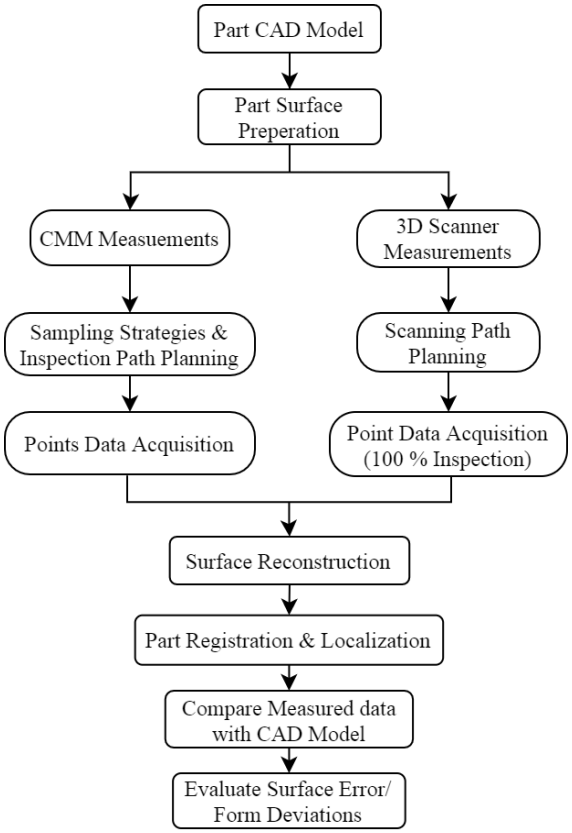

Fig. 3. Flow-chart of the inspection process.

All nine samples obtained after finish milling operation are inspected with both CMM and 3D scanner. The concept of form error is used to examine the part surface quality after machining. The articulated CMM and 3D Scanner set-up from Faro (Model: Quntum-S) is employed for measurement and inspection is shown in Fig. 2 (a)-(c). This is a 6-axis device consisting of various components and controls such as base color, probe, tubes, buttons, storage hook, etc. Three single point articulation tests are performed as per ISO 10360-12 to calibrate this device ensuring its accuracy and repeatability. Both the accuracy and repeatability of not-contact inspection is 35 μm and for contact inspection it is 34 μm and 24 μm respectively. Sample preparation and inspection planning are the two essential

steps before starting the actual measurement process. The other essential elements as probe selection, path generation, part holding/fixing device and application software, etc., are significant to ensure the inspection accuracy. The part surface is gently cleaned with cotton using acetone and being the part non-magnetic, it is fixed with glue. A developer spray 'CDK 30' that conforms to IS 3658 is applied over the part surfaces before scanning to ensure full data capture reducing losses due to scattering of the laser beam. Li and Lie implemented a rational approach to determine the probing points by combining both the scanner and CMM based measurements. The point cloud acquired through laser scanning is statistically analyzed to get the optimal model structure. The number of optimum probing points and their locations are thus identified based on this model structure considering the uncertainties to enhance speed and accuracy of measurement [25].

The process flowchart of inspection is given in Fig. 3 that employed both CMM and Laser scanner. Except for the sampling strategy, the procedure (steps involved) for both the devices are similar. With CMM, a definite number of data points are captured unlike 3D scanner, where the entire part is scanned (100% inspection), eliminating the need to define sampling strategy that makes inspections much faster compared to CMM [19]. In the latter case, a part surface is scanned employing a laser scanner with a stand-off distance of 80 mm and point grid spacing of 0.3 mm. In case of CMM, adequate sampling points are collected to make a trade-off between sampling speed and accuracy of surface representation. A free-form surface consisting 'n' ($n_u \times n_v$) control points, essentially require '$n \times 10$' measurement points to be acquired on the surface [25]. Accordingly, in this study, a total of 80 sampling points is collected randomly with a probe of 3 mm dia. to ensure accuracy and reliability of measurement. In random sampling, each sample point has an equal probability of being selected, which provides more authentic information about the chosen parameters. Further, more sampling points are considered along the longitudinal direction and the regions having more (abrupt) variations in surface profile to enhance the inspection quality [10].

3. Results and Discussions

Once adequate data points are collected, the other significant elements such as precise surface generation (reconstruction), part registration and localization, surface fitting and comparison that determine the quality of surface evaluation are executed in Delcam Power Inspect software. Part registration and localization is the mechanism by which a measurement coordinate system is fitted to design coordinate system to establish compatibility between two systems. The measurement points are transferred from the measurement coordinate system to the design coordinate system to facilitate the comparison between measured and CAD surfaces [26, 27]. Makem et al. verified the effectiveness of commonly used

part registration and localization techniques like Iterative Closest Point (ICP), 3–2–1 registration model in a virtual inspection of aero-engine blades with finite element (FE)-based simulations [26]. In another study, the authors developed an intelligent approach (software and hardware) for part registration as an effective and low-cost alternative to the traditional methods. The approach employs arbitrary axis rotation technique together with the k-d tree structure for point data matching and effectively verified for complex blade surfaces [27]. In 3D scanner measurements, the surface details captured in terms of point data are transferred to STL format which then used for digitizing and comparing the measured surface with CAD model. Several ideal shapes/features based on the acquired point data can be defined as a reference geometric feature in a software domain. Here, the point data acquired from part surfaces and 'Free-form alignment' feature is used to generate the surface. Subsequently, this surface is superimposed to CAD surface i.e., accurate registration is achieved with 'Best fit model' technique.

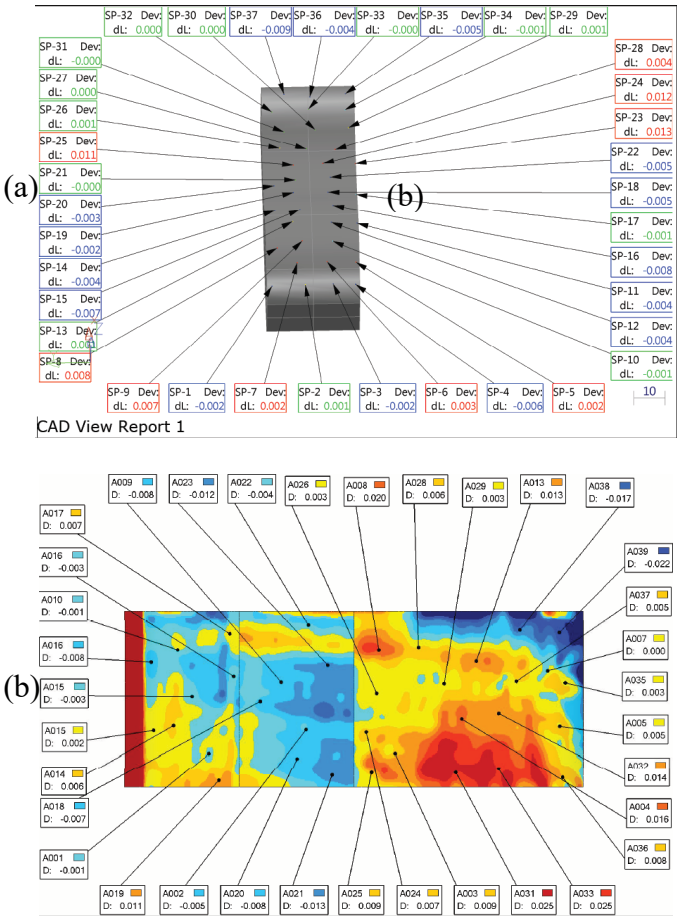

Fig. 4. Surface deviation evaluated with (a) CMM and (b) 3D Scanner.

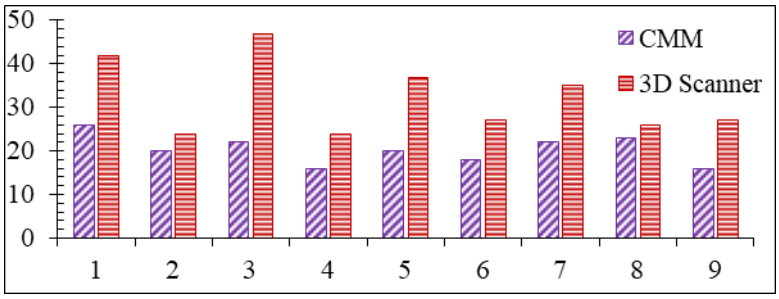

Fig. 5. Peak to valley distance (in micrometer) obtained for nine samples.

The surface deviations measured with CMM and 3D scanner for a sample are shown in Fig. 4. Different statistical parameters like peak to valley distance, average and standard deviations are computed based on the point cloud data obtained and plotted in the form of normal distribution (ND) curves. The values of these parameters for all nine parts are enlisted in Table 2. The range of measurement data underlines the total margin between two extreme surface deviation values (maximum scallop height + gauging depth) that encloses all the measurement points. Range is the peak to valley distance calculated over a surface and the average deviation is the average of all 35 readings. These parameters are expressed in terms of discrete values that merely specify the 'accuracy' of inspection process. However, along with accuracy, another significant index of inspection quality is 'measurement precision' that describes the spread or distribution of the data. In this study, a statistical parameter, standard deviation that measures the average degree to which each data point differs from a mean value or nominal model, is used to determine the 'precision.' The point data distribution is further presented as ND plots in the form of a bell-shaped curve considering mean, median and mode of the data.

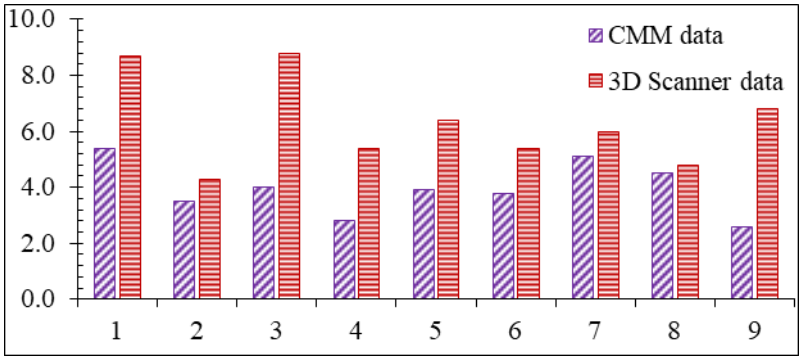

Fig. 6. Average deviations (in micrometer) for nine samples.

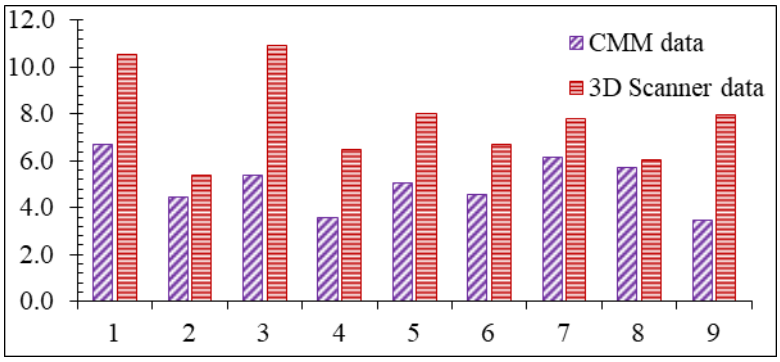

Fig. 7. Standard deviations (in micrometer) of the measurement data for nine samples.

The average deviations and standard deviations of form errors are evaluated based on measurement data. The process accuracy is evaluated by comparing peak to valley distances (deviation range) and average deviations for nine samples as plotted in Figs. 5 and 6. Both these parameters exhibit similar trends that emphasize better accuracy of CMM measurements over 3D scanner. But, the peak to valley distances and average deviations from CMM for all nine experiments are smaller compared to 3D scanner values.

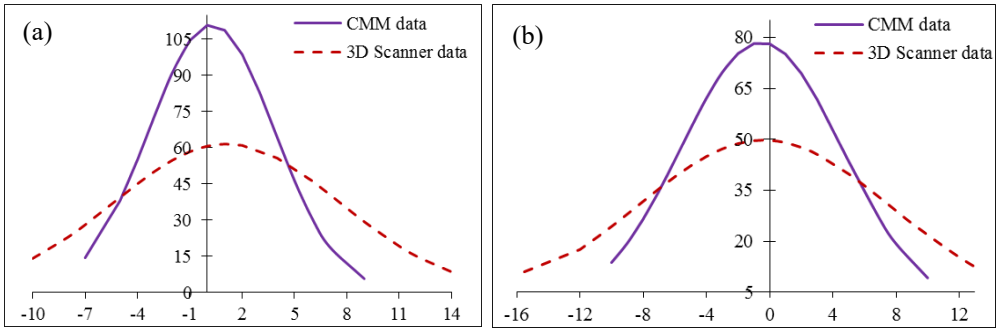

Fig. 8. Normal distribution (ND) curves of surface deviation (in micrometer) for (a) 4th and (b) 5th samples.

The standard deviations of form error for nine samples obtained with both the devices are compared in Fig. 7, which illustrates that the standard deviation of CMM measurements is smaller as compared to those of 3D scanner. The ND curves for CMM data plotted in Fig. 8 depicts higher peak and narrow range compared to scanner data. These curves evidence that CMM data is more uniformly distributed about the mean line. These curves highlight the importance of standard deviation as 68.3 % data points fall within ± 1s, while 95.5 % data points fall within ± 2*s* region of these curves. E.g., for sample 4 (ref. Table 1 and Fig. 8 (a)) standard deviation of CMM data and 3D scanner are 3.59 and 6.46 micrometer respectively. Accordingly, 95.5 % of CMM data would fall within ± 7.18 µm region while 95.5 % of scanner data would fall within ± 12.92 µm region that evidence high precision of CMM measurements. The bell-shaped curves also

validate the trends observed for standard deviations for all the samples. Hence, high accuracy and precision of CMM is obtained over 3D scanner.

4. Conclusions

The free-form parts finished with a ball-end mill are inspected using articulated CMM and 3D scanner. This study discusses a simple statistical approach to evaluate the inspection data in terms of parameters like average deviation, peak to valley distance, and standard deviation of the form deviation.

- The results are analyzed and plotted to compare the accuracy and precision of the inspection process. Some of the specific conclusions of this study are, the average deviations and peak to valley distance obtained with CMM (2.6 to 5.4 μm and 16 to 26 μm) are smaller than the 3D scanner (4.3 to 8.8 μm and 24 to 47 μm), ensuring higher accuracy of CMM.
- Similarly, the standard deviations of CMM (3.5 to 6.7 μm) are lesser than 3D scanner (5.4 to 10.9 μm) emphasizing higher precision of CMM measurements compared to 3D scanner. The normal distribution (ND) curves also validated this trend (with higher peak and narrow range) as CMM data is more uniformly distributed.
- The scanner-based inspections are prone to measured data loss in reflection, absorption, and dispersion, etc., which deteriorates the accuracy and precision of inspection. However, 3D scanner measurements featured with 100 % sampling (eliminating sampling strategy selection) are faster than CMM and best suitable for reverse engineering applications.

REFERENCES

[1] *R.A. Mali, R. Aiswaresh, T.V.K. Gupta*, The influence of tool-path strategies and cutting parameters on cutting forces, tool wear and surface quality in finish milling of Aluminium 7075 curved surface, The International Journal of Advanced Manufacturing Technology. 108 (2020) 589–601.

[2] *X.J. Jiang, P.J. Scott*, Advanced Metrology: Freeform Surfaces, 1st ed., Academic Press, 2020.

[3] *R.A. Mali, T.V.K. Gupta, J. Ramkumar,* A comprehensive review of free-form surface milling– Advances over a decade, J Manuf Process. 62 (2021) 132–167.

[4] *Y. Li, P. Gu,* Free-form surface inspection techniques state of the art review, Computer-Aided Design. 36 (2004) 1395–1417.

[5] *G. Mansour,* A developed algorithm for simulation of blades to reduce the measurement points and time on coordinate measuring machine (CMM), Measurement. 54 (2014) 51–57.

[6] *S.H. Mian, A.M. Al-Ahmari*, Application of the sampling strategies in the inspection process, Proc Inst Mech Eng B J Eng Manuf. 231 (2017) 565–575.

[7] *A. Wójcik, M. Niemczewska-Wójcik, J. Sladek*, Assessment of free-form surfaces' reconstruction accuracy, Metrology and Measurement Systems. 24 (2017) 303–312.

[8] *G. Fu, B. Sheng, R. Luo, X. Lu,* Research on on-machine measurement of machining error based on T-spline surface reconstruction, Meas Sci Technol. 32 (2021) 115028.

[9] *G. Rajamohan, M. s Shunmugam, G.L. Samuel*, Effect of probe size and measurement strategies on assessment of freeform profile deviations using coordinate measuring machine, Measurement. 44 (2011) 832–841.
[10] *J. Zahmati, H. Amirabadi, V. Mehrad,* A hybrid measurement sampling method for accurate inspection of geometric errors on freeform surfaces, Measurement. 122 (2018) 155–167.
[11] *E. Uhlmann, A.J. Abackerli, K. Schützer, H.A. Lepikson, A.L. Helleno, M.C.O. Papa, E.G. del Conte, J. Mewis,* Simulation and analysis of error impact on freeform surface milling, The International Journal of Advanced Manufacturing Technology. 70 (2014) 607–620.
[12] *V. Mehrad, D. Xue, P. Gu,* Inspection of freeform surfaces considering uncertainties in measurement, localization and surface reconstruction, Meas Sci Technol. 24 (2013) 085008.
[13] *S. Son, H. Park, K.H. Lee,* Automated laser scanning system for reverse engineering and inspection, Int J Mach Tools Manuf. 42 (2002) 889–897.
[14] *M. Mahboubkhah, M. Aliakbari, C. Burvill*, An investigation on measurement accuracy of digitizing methods in turbine blade reverse engineering, Proc Inst Mech Eng B J Eng Manuf. 232 (2016) 1653–1671.
[15] *A. Gameros, L. Chiffre, H. Siller, J. Hiller, G. Genta*, A reverse engineering methodology for nickel alloy turbine blades with internal features, CIRP J Manuf Sci Technol. 9 (2015) 116–124.
[16] *B. Li, F. Li, H. Liu, H. Cai, X. Mao, F. Peng*, A measurement strategy and an error-compensation model for the on-machine laser measurement of large-scale free-form surfaces, Meas Sci Technol. 25 (2013) 15204.
[17] *A. Contri, P. Bourdet, C. Lartigue*, Quality of 3D digitised points obtained with non-contact optical sensors, CIRP Annals. 51 (2002) 443–446.
[18] *L. Li, D. Xu, L. Niu, Y. Lan, X. Xiong*, A path planning method for a surface inspection system based on two-dimensional laser profile scanner, Int J Adv Robot Syst. 16 (2019) 1–13.
[19] *K.H. Lee, H. Park*, Automated inspection planning of free-form shape parts by laser scanning, Robot Comput Integr Manuf. 16 (2000) 201–210.
[20] *Y. Chen, N. Shang*, Comparison of GA, ACO algorithm, and PSO algorithm for path optimization on free-form surfaces using coordinate measuring machines, Engineering Research Express. 3 (2021) 045039.
[21] *A. Isheil, J.-P. Gonnet, D. Joannic, J.-F. Fontaine*, Systematic error correction of a 3D laser scanning measurement device, Opt Lasers Eng. 49 (2011) 16–24.
[22] *M.H. M Nashman, Tsai Hong Hong, William G. Rippey*, An Integrated Vision Touch-Probe System for Dimensional Inspection Tasks, in: Proceedings of the SME Applied Machine Vision' '96 Conference, The machine vision association of the socity of manufaturing engineers, Cincinnati, 1996: pp. 1–8.
[23] *L. Mu, Z. Yin, Y. Xiong*, A multisensor based on machine inspection approach for freeform surfaces, in: Proceedings 2011 International Conference on Transportation, Mechanical, and Electrical Engineering (TMEE), IEEE, Changchun, 2011: pp. 2166–2169.
[24] *M.C. Santos, A.R. Machado, W.F. Sales, M.A.S. Barrozo, E.O. Ezugwu*, Machining of aluminum alloys: a review, The International Journal of Advanced Manufacturing Technology. 86 (2016) 3067–3080.
[25] *Y.F. Li, Z.G. Liu*, Method for determining the probing points for efficient measurement and reconstruction of freeform surfaces, Meas Sci Technol. 14 (2003) 1280–1288.
[26] *J.E. Makem, H. Ou, C.G. Armstrong*, A virtual inspection framework for precision manufacturing of aerofoil components, Computer-Aided Design. 44 (2012) 858–874.
[27] *J. Tam, K. Yu, R. Sun*, Integrated computer-aided verification of turbine blade, Comput Aided Des Appl. 12 (2015) 1–12.